NOAA Technical Memorandum OAR PMEL-124

NOAA TIME SEATTLE TSUNAMI MAPPING PROJECT: PROCEDURES, DATA SOURCES, AND PRODUCTS

Vasily V. Titov[1]
Frank I. González[2]
Harold O. Mofjeld[2]
Angie J. Venturato[1]

[1]Joint Institute for the Study of the Atmosphere and Ocean (JISAO), Seattle, WA

[2]Pacific Marine Environment Laboratory, Seattle, WA

Pacific Marine Environmental Laboratory
Seattle, WA
September 2003

UNITED STATES DEPARTMENT OF COMMERCE

Donald L. Evans
Secretary

NATIONAL OCEANIC AND ATMOSPHERIC ADMINISTRATION

VADM Conrad C. Lautenbacher, Jr.
Under Secretary for Oceans and Atmosphere/Administrator

Oceanic and Atmospheric Research Laboratories

Richard D. Rosen
Director

NOTICE

Mention of a commercial company or product does not constitute an endorsement by NOAA/OAR. Use of information from this publication concerning proprietary products or the tests of such products for publicity or advertising purposes is not authorized.

Contribution No. 2572 from NOAA/Pacific Marine Environmental Laboratory

For sale by the National Technical Information Service, 5285 Port Royal Road
Springfield, VA 22161

Contents

List of Figures

List of Tables

NOAA TIME Seattle Tsunami Mapping Project: Procedures, data sources, and products

Vasily V. Titov[1], Frank I. González[2], Harold O. Mofjeld[2], and Angie J. Venturato[1]

1. Introduction

This report describes the project of the NOAA Center for Tsunami Mapping Efforts (TIME) to model and map potential tsunami inundation along the Puget Sound shores of Seattle, Washington (Fig. 1). The source of the scenario tsunami is a major (magnitude 7.3) earthquake of the Seattle Fault. The goal of this work is to provide data for creating tsunami inundation maps for these areas. The maps are prepared as part of the National Hazard Mitigation Program to aid local governments in designing evacuation plans for areas at risk from potentially dangerous tsunamis. The details of the tsunami generation are extremely important, since the tsunami inundation area is in close proximity to the tsunami source. Hence the latest scientific evidence about the Seattle Fault structure and seismicity is employed to design a tsunami source scenario for this study. We apply a high-resolution tsunami inundation model to estimate details of the runup on land near the Seattle shoreline.

2. Background

Recent advancements in geological and paleo-tsunami studies have identified the Seattle Fault Zone as a substantial seismic and tsunami hazard for the Seattle Area (Fig. 1). Scientists have collected compelling evidence about earthquakes and tsunami events originated on the Seattle fault (Gower *et al.*, 1985; Atwater and Moore, 1992; Johnson *et al.*, 1999; Bourgeois and Johnson, 2001; Brocher *et al.*, 2001; Blakely *et al.*, 2002). Estimates of the repeat period for a large event on this fault are not well established (probably, in millennia range). Nevertheless, the proximity to a large metropolitan area makes the risk from such an event very formidable and warrants thorough scientific assessment.

It is nearly certain that a tsunami will accompany a large rupture on the Seattle Fault. The geometry of the fault favors large vertical deformations of the seabed under Puget Sound, which would result in the displacement of a large amount of water. The disturbed water mass would then propagate as tsunami waves. The impact of the tsunami around Puget Sound can be estimated with numerical modeling. Previous modeling studies of the Seattle Fault tsunami have focused on reproducing the paleo-evidences of the tsunami of 1100 years ago. Walters and Takagi (1996) and Holmes

[1]Joint Institute for the Study of the Atmosphere and Ocean (JISAO), University of Washington, Box 354235, Seattle, WA 98195-4235

[2]NOAA/Pacific Marine Environmental Laboratory, 7600 Sand Point Way NE, Seattle, WA 98115

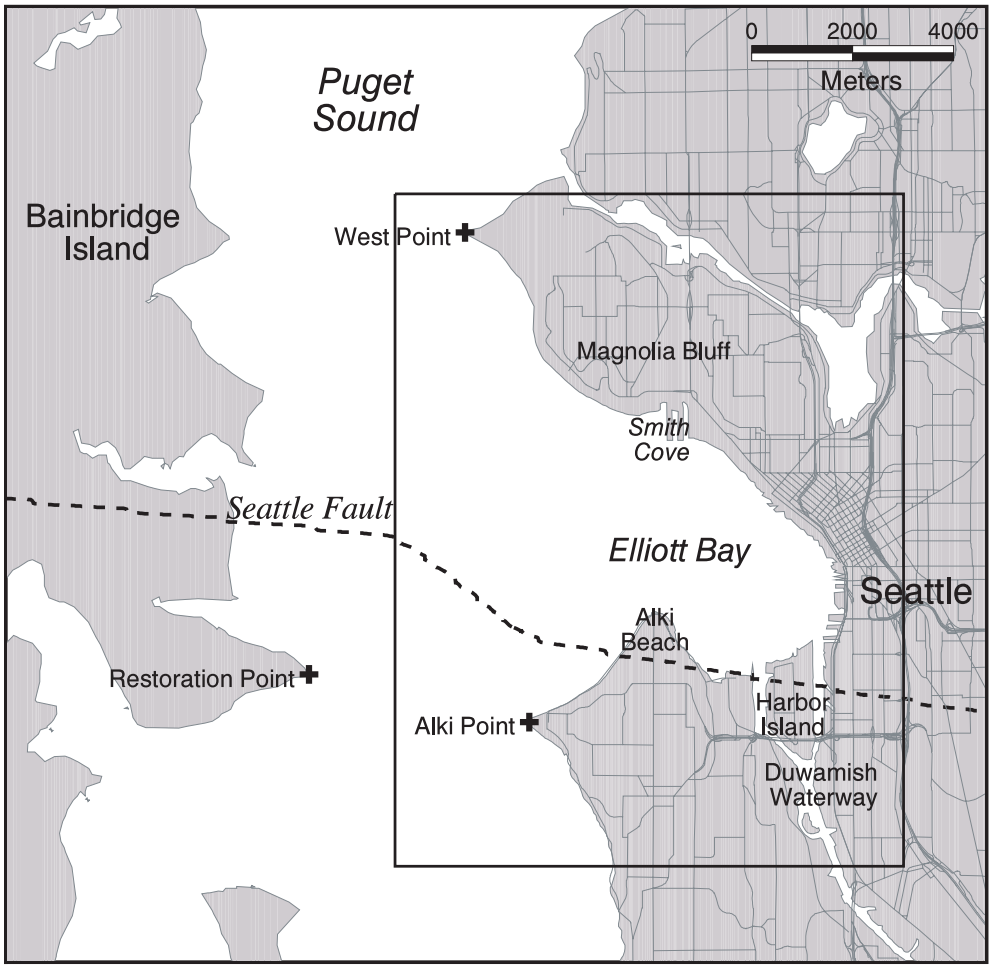

Figure 1: Study area of the Seattle Tsunami Mapping Project. Broken line shows surface signature of the Seattle Fault model. Black rectangle outlines the area for the high-resolution tsunami inundation modeling.

and Dinkelman (1993) have modeled the propagation of the tsunami around Puget Sound using a simplified source and a coarse numerical grid. They identified general patterns of tsunami propagation and offshore amplitudes of propagating waves around Puget Sound. Koshimura *et al.* (2002) have developed a refined model of the same event. They have reproduced much of the paleo-evidence of the tsunami in Cultus Bay with their inundation model. The source mechanism of their model is based on the interpretation of Pratt *et al.* (1997) of the Seattle Fault geometry.

3. Tsunami Source

The tsunami source for this study assumes wave generation by a rupture of the Seattle Fault. It is designed as a maximum credible event based on the

scientific evidence about the Fault geometry, seismicity, and field evidence for co-seismic displacements of the Fault.

Many details of the Seattle Fault are still poorly understood. A steady stream of new scientific information leads to continuous reassessment of the Seattle Fault structure and potential (e.g., Pratt *et al.*, 1997; Johnson *et al.*, 1999; Blakely *et al.*, 2002). The tsunami generation, however, depends only on the surface manifestation (the amount of vertical offset) of the internal fault rupture. Therefore, the internal fault geometry, though important, may not be as vital a constraint for the tsunami model as the vertical deformation evidence. The 900 A.D. earthquake on the Seattle fault produced uplifts of up to 7 m and subsidence of more than 1 m, based on the shoreline displacement data (e.g., Bucknam *et al.*, 1999; ten Brink *et al.*, 2002). This earthquake generated a tsunami known from several deposits at West Point (in Seattle), Cultus Bay (at the south end of Whidbey Island) and the Snohomish River delta near Everett (Atwater and Moore, 1992; Bourgeois and Johnson, 2001). Hence, this vertical deformation data (+7 meters at Restoration Point, +4 meters at Alki Point and at least –1 meter at West Point) that is known to produce a tsunami from the Seattle Fault is used here as a main constraint for a credible tsunami source model.

The near-surface structure of the Seattle Fault Zone is fairly well determined from the field evidence, seismic reflection studies, aeromagnetic data, and gravity anomalies (e.g., Bucknam *et al.*, 1992; Pratt *et al.*, 1997; Brocher *et al.*, 2001; Calvert and Fisher, 2001; Blakely *et al.*, 2002). Koshimura *et al.* (2002) have utilized this surface configuration for their source of the 900 A.D. tsunami simulation. Our study uses a similar surface signature for the model source—six sub-faults with surface edges following the northern strand of the Seattle Fault Zone (Fig. 1).

The data about the internal structure of the Seattle Fault is not as straightforward to interpret as its surface configuration and is subject to many different interpretations. Pratt *et al.* (1997) suggested a wide shallow dipped fault (20°) that extends from 16 km deep up to 6 km from the surface, which breaks to the surface with a steeper (35°–40°) narrow strand. This was the model adopted by Koshimura *et al.* (2002). Later interpretations favor steeper and deeper faults extending from depths of 20–28 km to the surface with dip angles varying from 40° to 80° (Brocher *et al.*, 2001; Calvert and Fisher, 2001). Others suggest more complex near surface structure with secondary faults near the surface (ten Brink *et al.*, 2002). Brocher *et al.* (2001) also suggest a link between seismicity of the Seattle Fault and the Tacoma Fault to the south when one fault may trigger movement on the other.

Taking into account the uncertainties of the Seattle Fault data and differences in interpretations, we have chosen an unambiguous fault model that is in general agreement with modern interpretations and, most importantly, can accommodate the measured vertical displacements of the tsunamigenic event of 1100 years ago. We assume movement only at the Seattle Fault Zone in this scenario. Our model has a single fault uniformly dipping at a 60° angle down to 17.3 km along all its length. The 60° dip angle is within the uncertainty range of many recent fault models (ten Brink *et al.*, 2002;

Table 1: Sub-fault parameters (from West to East).

Sub-Fault	F1	F2	F3	F4	F5	F6
Length	15.2 km	6.3 km	8.9 km	3.3 km	11.5 km	14.9 km
Width	20 km	20 km	20 km	20 km	20 km	20 km
Strike	87.9°	86.6°	96°	128.8°	99.3°	81°
Dip	60°	60°	60°	60°	60°	60°
Displacement	1 m	1 m	12 m	11 m	4 m	1 m

Table 2: Comparison of the model source vertical displacements with shoreline uplift data.

Displacements	Model	Observations
Alki Point	3.9 m	4 m
Restoration Point	7.1 m	7 m
West Point	-1.3 m	-1 ± 0.5 m

Brocher *et al.*, 2001; Calvert and Fisher, 2001; Blakely *et al.*, 2002). The lower depth of the fault is also a subject of active debate. Different hypotheses put the low boundary of the fault anywhere from 12 to 28 km deep. Then again, the deeper part of the fault does not contribute as much to the surface deformation. Therefore, the depth of the low boundary, though important for the geophysical understanding of the fault structure, is not significant for the tsunami generation.

The geophysical data suggest that the Seattle Fault is capable of generating an earthquake of M_w greater than 7, with maximum estimates of M_w 7.6–7.7 (Pratt *et al.*, 1997; Koshimura *et al.*, 2002). We have chosen a mid-range of magnitude estimates for the model source $M_w = 7.3$. Using this magnitude as a constraint, we have distributed the slip values among the sub-faults to reproduce vertical displacement estimates of the 900 A.D. event. The resulting slip distribution and sub-fault's parameters are listed in Table 1.

The maximum slip values for our source, though large, are consistent with data for similar type thrust-earthquakes published elsewhere. A well-documented thrust fault of the 1999, M_w 7.5, Chi-Chi earthquake in Taiwan, for example, produced up to a 20 m slip in a small area of the fault (within 5 $\times$ 5 km^2), which, in turn, generated 11 m vertical offset at the surface above this asperity (e.g., Zhang *et al.*, 2003).

Table 2 shows comparison of the computed vertical displacements with the most reliable estimates of the 900 A.D. earthquake offsets at three locations.

Vertical displacements for this model were computed using Okada's formulation of the elastic deformation approximation (Okada, 1985). Figure 2 shows contours of the computed vertical deformations due to the rupture of the assumed fault configuration from Table 1. The identical displacement of the sea surface (color-coded on Fig. 2 as red-uplift, dark blue-subsidence) above the deformed crust would propagate along Puget Sound as a tsunami wave, and is used as initial conditions for the tsunami propagation and inundation model.

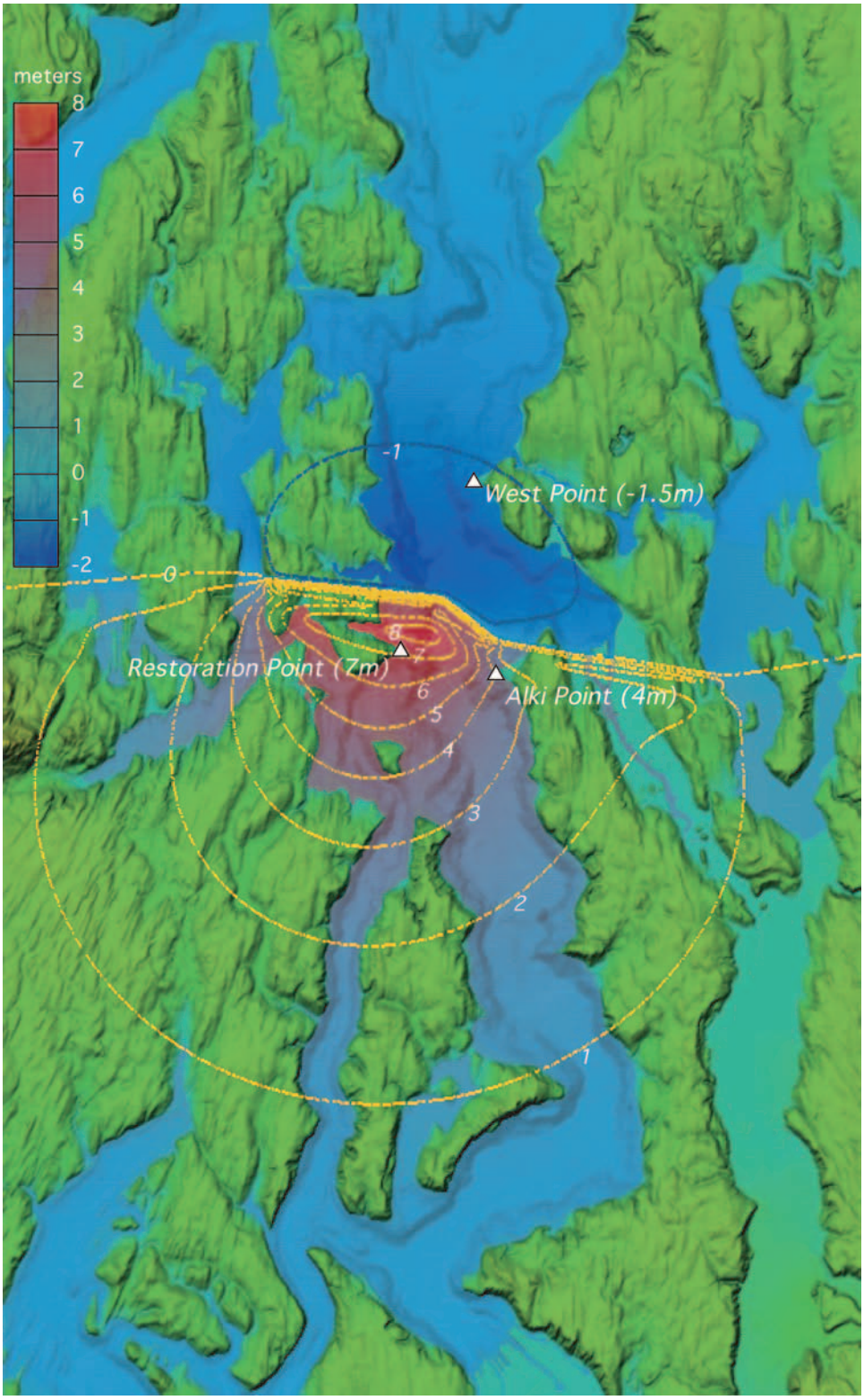

Figure 2: Distribution of computed vertical deformations used as a tsunami source for the inundation study. Contours show deformation of the earth crust due to rupture of the model Seattle Fault. Resulting sea-surface deformation is shown color-coded in red (uplift) and blue (subsidence). White triangles show locations of historical deformation measurements.

4. Tsunami Model

The tsunami propagation around Puget Sound and wave inundation on dry land is simulated with the MOST numerical model (Titov and González, 1997; Titov, 1997; Titov and Synolakis, 1995). MOST is a finite-difference numerical algorithm based on the long wave approximation. It solves numerically the non-linear shallow water wave equations written in spherical coordinates as follows:

$$
\begin{aligned}
h_t &+ \frac{(uh)_\lambda + (vh\cos\phi)_\phi}{R\cos\phi} = 0 \\
u_t &+ \frac{uu_\lambda}{R\cos\phi} + \frac{vu_\phi}{R} + \frac{gh_\lambda}{R\cos\phi} = \frac{gd_\lambda}{R\cos\phi} + fv - \frac{C_f}{h}\,|u|\,u \\
v_t &+ \frac{uv_\lambda}{R\cos\phi} + \frac{vv_\phi}{R} + \frac{gh_\phi}{R} = \frac{gd_\phi}{R} - fu - \frac{C_f}{h}\,|v|\,v,
\end{aligned}
$$

where λ is longitude, ϕ is latitude, $h = h(\lambda,\phi,t) + d(\lambda,\phi,t), h(\lambda,\phi,t)$ is the amplitude, $d(\lambda,\phi,t)$ is the undisturbed water depth, $u(\lambda,\phi,t), v(\lambda,\phi,t)$ are the depth-averaged velocities in the longitude and latitude directions, respectively, g is the gravity acceleration, f is the Coriolis parameter ($f = 2\omega\sin\phi$) and R is the Earth radius, $C_f = gn^2/h^{1/3}$ (n is the Manning coefficient). In the MOST model, these equations are solved numerically using a splitting method similar to that described by Titov (1997).

The MOST model has been extensively tested against various laboratory experiments (Titov and Synolakis, 1998, 1996) and verified by successfully reproducing field data for many historical tsunamis (Yeh *et al.*, 1995; Titov and Synolakis, 1997, 1998; Titov and González, 1997).

The MOST model was applied for the Seattle simulation without Coriolis terms. This effect—small even for long-distance tsunami propagation (e.g., Kowalik and Whitmore (1991))—is negligible at short distances, such as the ones in the Puget Sound modeling study. The Manning's formulation of the bottom friction is used for the inundation computation with constant Manning coefficient $n = 0.025$.

The topography used for the simulation does not include buildings and other structures, so-called "bald earth" digital elevation model (DEM). These obstacles may change and decrease inundation estimates, especially for large flat areas. One way of accounting for that increased dissipation in the long-wave model is the use of a greater bottom friction parameter (Fujima, 2001). However, there are not enough data and scientific studies to choose the proper friction coefficients to account for large structures. In the absence of proven scientific estimates, we have chosen to use a standard engineering value for the Manning parameter corresponding to mildly rough surfaces ($n = 0.025$). That approach gives credible conservative estimates of the tsunami inundation.

To reproduce the correct wave dynamic during the inundation computations, a high-resolution grid is required. The MOST model is designed to use several nested computational grids to telescope into the high-resolution inundation area. These high-resolution computations require a high-quality

bathymetry and topography data merged into one computational grid. Appendix A describes the procedure to develop DEMs for the Seattle inundation modeling. It also lists the sources of the bathymetry and topography used to create the DEM.

5. Discussion of Modeling Results

5.1 Offshore Dynamics

The Seattle Fault tsunami source creates a sharp bottom dislocation along the fault surface (Fig. 2). There is an upward displacement to the south of the Fault and a lesser downward displacement to the north. That dislocation goes across Puget Sound from Bainbridge Island to Alki Beach and further east crosses both Duwamish Waterways. The corresponding gradient of the water surface forms the initial wave front of the tsunami. The largest amplitudes are generated at Puget Sound between Bainbridge and Alki Point. The wave from that portion of the fault propagates directly toward the shores of Magnolia Bluff and into Elliott Bay. The first wave crest forms a bore with amplitudes above 6 m before reaching the Magnolia Bluff shore only 2 min 20 sec after generation. Within half a minute after that, this wave crest reaches all the shores around Elliott Bay. The south shores of Elliott Bay are not inundated by the first crest, not until a large wave reflected from the northern coasts reaches Harbor Island about 5 min after the earthquake (Fig. 3).

5.2 Inundation Details

The model predicts extensive inundation by the tsunami waves in some areas around Elliott Bay. Here, we discuss various aspects of the computed inundation dynamic and contributing factors that explain these results.

The maximum amplitudes of tsunamis approaching shores of Elliott Bay are very similar around the Bay, fluctuating around 6 m. Significant differences in the inundation amplitudes and penetration distances are, therefore, explained mainly by variations of local topography near the shore. Inspection of the topography data reveals that some coastal sites have a very flat and low profile, with large areas near the shore not more than 5–7 m above mean high water. One of such areas includes Harbor Island, adjacent port facilities, and industrial areas that are built on filled land. Another low-lying area runs north from Smith Cove. The model predicts large inundation distances (up to 1 mile) at both of these locations, but not the largest vertical amplitudes (Fig. 4).

The highest vertical runup (above 10 m) is computed at steep southwest bluffs of Magnolia Bluff and second highest at Alki Beach, east of Alki Point (Fig. 4). In both areas, the inundation distances are very small. Such trends are predictable and expected. Long waves, like tsunamis, tend to flood the entire area below its shoreline amplitude. Over flat topography such waves lose their energy via bottom friction, and the inundation depths then slowly decrease over long penetration distances.

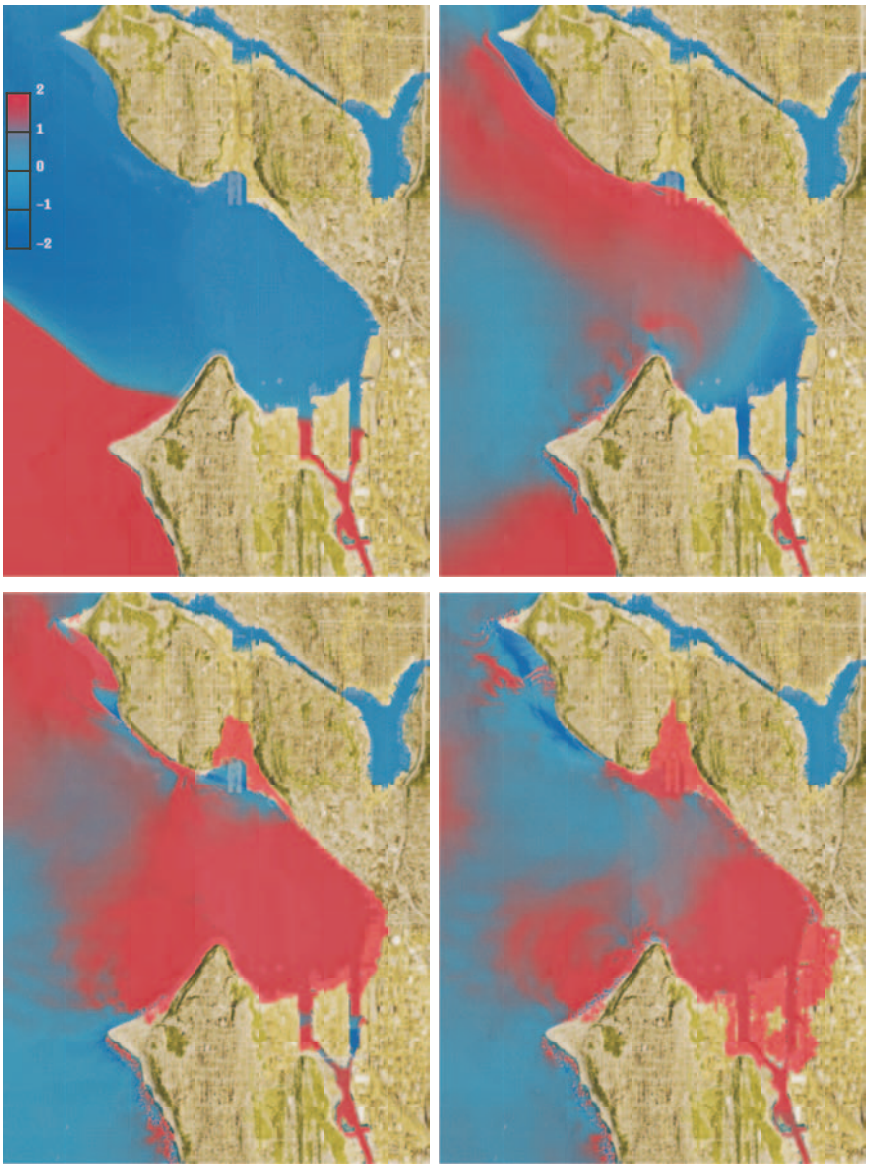

Figure 3: Snapshots of model tsunami propagation in Elliott Bay. Red color indicates positive wave amplitudes above Mean High Water (MHW), blue is negative (below MHW).

Many historical tsunamis demonstrated similar inundation patterns. For example, the 2001 Peru tsunami penetrated up to 1 mile inland over flat agricultural fields near Camana (Okal *et al.*, 2002). Steep beaches, on the other hand, would create nearly perfect reflection, effectively doubling the amplitudes of incoming long waves. It is also confirmed by field data of historical events. The 1997 Okushiri tsunami produced the highest runup at steep cliffs on the west coast of Okushiri Island, which was later reproduced by the MOST model simulation (Titov and Synolakis, 1997).

Figure B7 shows maximum computed inundation depths that illustrate

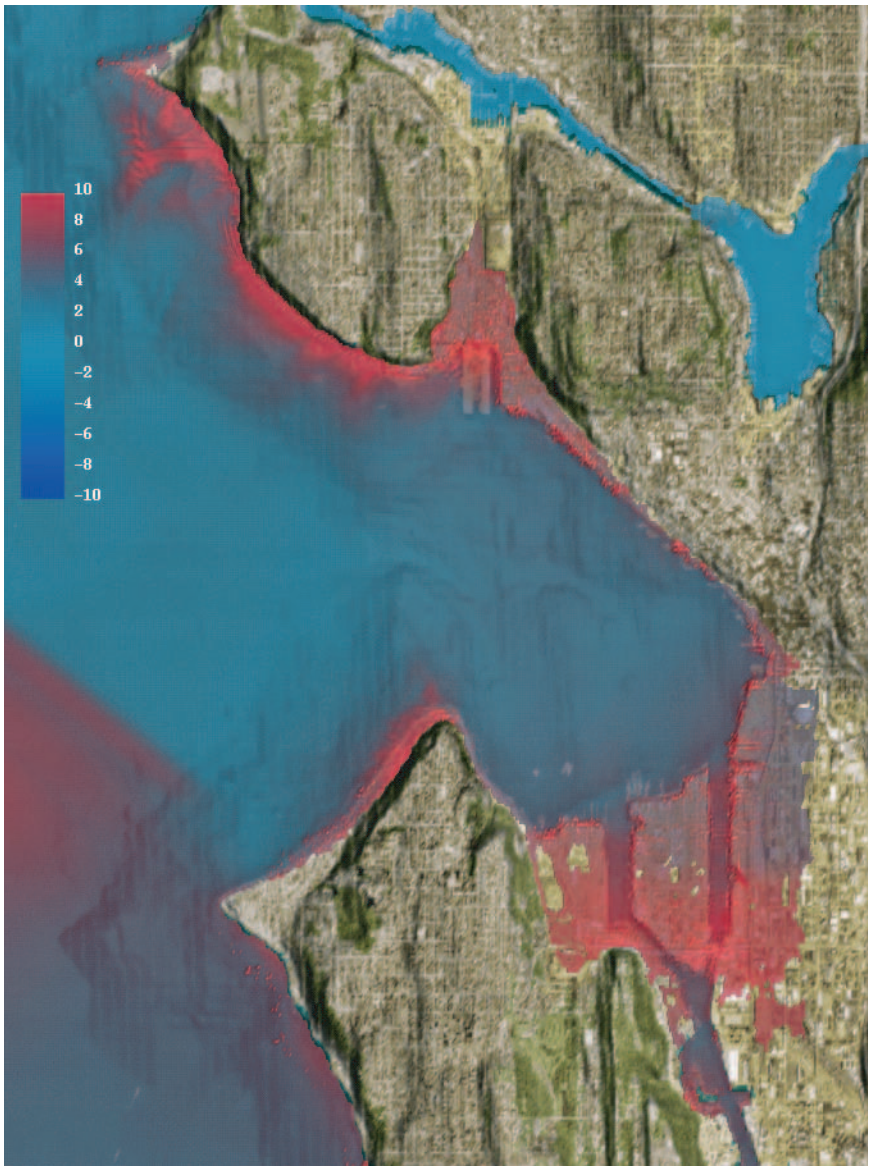

Figure 4: Distribution of the maximum computed wave heights in Elliott Bay and runup at Seattle coastlines (in meters above MHW).

those inundation patterns. It demonstrates the decrease of flow depths away from a shoreline for inundation at large flat areas around Harbor Island and near Smith Cove, while higher inundation amplitudes are computed at steep shores with short inundation distances at SW Magnolia Bluff and at eastern Alki Beach. To present the internal structure of computed inundation, we have decided to use zones of inundation based on the computed flow depth: low, medium, and high inundation (Fig. B9). The zoned inundation map provides a more complete and informative representation of the flooding than just a single maximum inundation line.

These modeling results are intended for development of the tsunami in-

undation maps for the Seattle Area. The numerical data from the described simulation is provided to Washington State officials for development of the inundation maps and additional products. Appendix B lists all modeling products prepared as a result of this study.

6. Acknowledgments

This research is funded by the National Tsunami Hazard Mitigation Program via a grant from the Washington State Emergency Management Division. We thank George Crawford, Timothy Walsh, Craig Weaver and many other researchers for helpful discussions regarding Seattle Fault source.

This publication is partially funded by the Joint Institute for the Study of the Atmosphere and Ocean (JISAO) under NOAA Cooperative Agreement No. NA67RJ0155, Contribution # 1006.

References

Atwater, B.F., and A.L. Moore (1992): A tsunami about 1000 years ago in Puget Sound, Washington. *Science*, *258*, 1614–1617.

Blakely, R.J., R.E. Wells, C.S. Weaver, and S.Y. Johnson (2002): Location, structure, and seismicity of the Seattle Fault Zone, Washington: Evidence from aeromagnetic anomalies, geologic mapping, and seismic-reflection data. *Geol. Soc. Am. Bull.*, *114*(1), 169–177.

Bourgeois, J., and S.Y. Johnson (2001): Geologic evidence of earthquakes at the Snohomish Delta, Washington, in the past 1200 yr. *Geol. Soc. Am. Bull.*, *113*, 482–494.

Brocher, T.M., T. Parsons, R.J. Blakely, N.I. Christensen, M.A. Fisher, R.E. Wells, and the SHIPS Working Group (2001): Upper crustal structure in the Puget Lowland, Washington: Results from the 1998 seismic hazard investigation in Puget Sound. *J. Geophys. Res.*, *106*(B7), 13,541–13,564.

Bucknam, R.C., E. Hemphill-Haley, and E.B. Leopold (1992): Abrupt uplift within the past 1700 years at southern Puget Sound, Washington. *Science*, *258*, 1611–1614.

Bucknam, R.C., B.L. Sherrod, and G. Elfendahl (1999): A fault scarp of probable holocene age in the Seattle Fault Zone, Bainbridge Island, Washington. *Seismol. Res. Lett.*, *70*(2), 233.

Calvert, A.J., and M.A. Fisher (2001): Imaging of the Seattle Fault Zone with high resolution seismic tomography. *Geophys. Res. Lett.*, *28*(12), 2337–2340.

Fujima, K. (2001): Long wave propagation on large roughness. In *Proceedings of International Tsunami Symposium*, Seattle, WA, 4–7 August 2003, 7–22.

Gower, H.D., J.C. Yount, and R.S. Crosson (1985): Seismotectonic map of the Puget Sound region, Washington. In *U.S. Geological Survey Miscellaneous Investigations Series*, (1 sheet), I-1613, scale 1:250,000, USGS, 15.

Holmes, M., and L. Dinkelman (1993): Modeling paleotsunamis in Puget Sound, Washington. Abstracts with Programs. *Geol. Soc. Am.*, *25*(1), 289–290.

Johnson, S.Y., S.V. Dadisman, J.R. Childs, and W.D. Stanley (1999): Active tectonics of the Seattle Fault and Central Puget Sound Washington—Implications for earthquake hazards. *Geol. Soc. Am. Bull.*, *111*(7), 1042–1053.

Koshimura, S., H.O. Mofjeld, F.I. González, and A.L. Moore (2002): Modeling the 1100 bp paleotsunami in Puget Sound, Washington. *Geophys. Res. Lett.*, *29*(20), 1948, doi: 10.1029/2002GL015170.

Kowalik, Z., and P. Whitmore (1991): An investigation of two tsunamis recorded at Adak, Alaska. *Sci. Tsunami Haz.*, *9*(2), 67–85.

Mofjeld, H.O., A.J. Venturato, V. Titov, F.I. González, and J.C. Newman (2002): Tidal datum distributions in Puget Sound, Washington, based on a tidal model. NOAA Tech. Memo. OAR PMEL-122 (PB2003-102259), NOAA, Pacific Marine Environmental Laboratory, 35 pp.

Okada, Y. (1985): Surface deformation due to shear and tensile faults in a half space. *Bull. Seismol. Soc. Am.*, *75*, 1135–1154.

Okal, E.A., L. Dengler, S. Araya, J.C. Borrero, B.M. Gomer, S. Koshimura, G. Laos, D. Olcese, M. Ortiz, M. Swensson, V.V. Titov, and F. Vegas (2002): Field survey of the Camaná, Peru tsunami of June 23, 2001. *Seismol. Res. Lett.*, *73*(6), 907–920.

Pratt, T.L., S. Johnson, C. Potter, W. Stephenson, and C. Finn (1997): Seismic reflection images beneath Puget Sound, western Washington State: The Puget lowland thrust sheet hypothesis. *J. Geophys. Res.*, *102*, 27,469–27,489.

ten Brink, U.S., P.C. Molzer, M.A. Fisher, R.J. Blakely, R.C. Bucknam, T. Parsons, R.S. Crosson, and K.C. Creager (2002): Subsurface geometry and evolution of the Seattle fault zone and the Seattle basin, Washington. *Bull. Seismol. Soc. Am.*, *92*, 1737–1753.

Titov, V.V. (1997): Numerical modeling of long wave runup. Ph.D. thesis, University of Southern California, Los Angeles, California, 141 pp.

Titov, V.V., and F.I. González (1997): Implementation and testing of the Method of Splitting Tsunami (MOST) model. NOAA Tech. Memo. ERL PMEL-112 (PB98-122773), NOAA, Pacific Marine Environmental Laboratory, 11 pp.

Titov, V.V., and C.E. Synolakis (1995): Modeling of breaking and nonbreaking long wave evolution and runup using VTCS-2. *J. Waterw. Port Coast. Ocean Eng.*, *121*(6), 308–316.

Titov, V.V., and C.E. Synolakis (1996): Numerical modeling of 3-D long wave runup using VTCS-3. In *Long Wave Runup Models*, World Scientific Publishing Co. Pte. Ltd., Singapore, 242–248.

Titov, V.V., and C.E. Synolakis (1997): Extreme inundation flows during the Hokkaido-Nansei-Oki tsunami. *Geophys. Res. Lett.*, *24*(11), 1315–1318.

Titov, V.V., and C.E. Synolakis (1998): Numerical modeling of tidal wave runup. *J. Waterw. Port Coast. Ocean Eng.*, *124*(4), 157–171.

Walters, R.A., and T. Takagi (1996): Review of finite element methods for tsunami simulation. In *Long-Wave Run Up Models*, H. Yeh, P. Liu, and

C. Synolakis (eds.), World Scientific, River Edge, NJ, 43–87.

Yeh, H., V.V. Titov, V. Gusyiakov, E. Pelinovsky, V. Khramushin, and V. Kaistrenko (1995): The 1994 Shikotan earthquake tsunami. *Pure Appl. Geophys.*, *144*(3/4), 569–593.

Zhang, W., T. Iwata, and K. Irikura (2003): Heterogeneous distribution of the dynamic source parameters of the 1999 Chi-Chi, Taiwan, earthquake. *J. Geophys. Res.*, *108*, doi: 10.1029/2002JB001889.

Appendix A: Bathymetry Data and Computational Grids

Procedure

The TIME Center has developed data grids for the Seattle inundation mapping project using the following five-step process:

- Data Collection
- Data Assessment
- Grid Computation
- Grid Assessment
- Product Delivery

The best available bathymetric and topographic data were obtained from government agencies. These sources are listed in the next section. The data were reformatted and then analyzed for quality using ESRI GIS software. Datasets were converted to the Universal Transverse Mercator Zone 10 projection and the North American Datum of 1983. The data were then corrected to a vertical datum of Mean High Water using tidal data obtained over a 19-year period (1960–1978) from the Seattle National Ocean Service water level station (station number 944-7130). Bathymetric data was corrected from Mean Lower Low Water, and topographic data was corrected from National Geodetic Vertical Datum of 1929. The mean values were calculated by the National Ocean Service using the 1960–1978 tidal epoch and were assumed constant throughout the Seattle model region. This approximation is accurate to within ±0.05 m along the Seattle shoreline (Mofjeld *et al.*, 2002).

A coastline file was generated based on governmental data sources and local knowledge of the Seattle Area. Some piers with open pile foundations were eliminated from the coastline data for inundation modeling purposes. Tsunami waves can freely propagate under these piled piers, therefore the inundation is better modeled without those piers as part of the reflective shoreline.

A combined bathymetric and topographic data grid was then generated using ArcInfo. Various datasets were combined using Triangulated Irregular Network modeling. The results were converted into a rectangular grid of 30-meter resolution. Two grids were generated from the original 30-meter grid: a subset of the 30-meter grid focusing on Elliott Bay and a 90-meter grid using a resampling technique.

The computed grid was analyzed for quality. Comparisons were made between the original datasets and the grid. Datums were verified and point errors were removed.

The grids were then converted into geographic coordinates for use by the MOST numerical model. The grids being distributed to Division of Geology and Earth Resources are in the State Plane Coordinate System of 1927, Zone 5626 with the North American Datum of 1927.

Table A1: Data sources used for grid development.

Media Source	Media	Data	Description
National Ocean Service (NOS)	Digital Elevation Model	30-meter NOS bathymetry digital elevation model	Bathymetric data obtained from 1934–1982 by NOS
National Geophysical Data Center (NGDC)	CD-ROM (GEODAS Version 4.1)	NOS Hydrographic Surveys	Bathymetric data from 1998 NOS hydrographic survey
USGS Open File Report OF01-266	ArcInfo Grid	4-meter NOS bathymetry digital elevation model	Bathymetric data from 2001 NOS hydrographic survey
University of Washington PRISM Project	ArcInfo Grid	10-meter topography digital elevation model	Topographic data obtained from the U.S. Geological Survey
City of Seattle	Arcview Point Shapefiles	2-foot contour topography of Seattle	Topographic data obtained in 1993 from aerial photogrammetry

Data Sources

The data sources for the grids are described in Table A1. The resolution of each data source varied from approximately 1–30 meters. Many sources were in different formats, which may lead to a small conversion error. The vertical accuracy of the data is based on the root mean square error; approximately 5% of depth for bathymetry and one-half of the contour interval for topography.

The data sources used for the DEMs are credited to the following groups:

- National Oceanic and Atmospheric Administration, National Geodetic Database Centers. Hydrographic Surveys, GEODAS Version 4.1 Software. Boulder, Colorado.
  Website reference: `http://www.ngdc.noaa.gov/mgg/bathymetry/relief.html`.
- National Oceanic and Atmospheric Administration, National Ocean Service. NOS Estuarine Bathymetry. Silver Spring, Maryland.
  Website reference: `http://mapfinder.nos.noaa.gov/`.
- U.S. Geological Society, Western Region Geology. Open File Report OF01-266. San Francisco, California.
  Website reference: `http://geopubs.wr.usgs.gov/open-file/of01-266/`.
- Washington State Geospatial Data Archive, University of Washington. U.S. Geological Survey 10-meter Digital Elevation Model. Seattle, Washington.
  Website reference: `http://duff.geology.washington.edu/data/raster/tenmeter/`.

Table A2: Grid summary.

Region	Name	Resolution	Extents (SW and NE corners)
Puget Sound	seattle90	90 meters	SW: −122.752, 47.035
			NE: −122.175, 48.124
Elliott Bay	seattle30	30 meters	SW: −122.454, 47.549
			NE: −122.321, 47.668

- City of Seattle, Seattle Public Utilities. City of Seattle Topography. Seattle, Washington.
  Website reference: `http://www.cityofseattle.net/util/.`
- National Oceanic and Atmospheric Administration, Center for Operational Oceanographic Products and Services, Water Level Station Information for Kodiak Island, Alaska. Silver Spring, Maryland.
  Website reference: `http://www.co-ops.nos.noaa.gov/.`
- Information about ESRI GIS software can be found on the Internet at `http://www.esri.com/.`

Products

Two grids are being delivered to the Division of Geology and Earth Resources. Each grid is described in Table A2. The grids are in ArcInfo exchange format and have the following parameters:

- Grid Generation Software: ArcInfo, Version 8.0.2
- Grid Algorithm: Triangulated Irregular Network
- Horizontal Datum: North American Datum of 1927
- Vertical Datum: Mean High Water
- Projection: State Plane Coordinate System of 1927, Zone 5626
- Units: feet
- Z Units: meters
- Grid accuracy is based on the level of detail of the source and the grid interval used to sample the source.

Appendix B: Modeling Products

Three vector files, nine raster grids, and an animation are included on a CD-ROM with this report.

Each product is summarized in Table B1. All files are in the ESRI ArcView 3.2 format and have the following parameters as requested by the Division of Geology and Earth Resources:

- Projection: State Plane Coordinate System
- Zone: 5626 (Washington South)
- XY Units: feet
- Z Units: meters (meters/second for speeds)
- Horizontal Datum: North American Datum of 1927
- Vertical Datum: Mean High Water

Each file has an associated gif image and metadata report. The vector files and raster grids are displayed in an ArcView 3.2 project file for easy access and distribution. The animation is in QuickTime format. A NOAA Technical Memorandum and model output will be distributed at a later date.

Table B1: Product summary.

Item	Name	Filename	Type	Image	Metadata	Resolution (m)
0	(a) Model Output (b) Animation (c) Documentation	seattle.qt	Quick-Time			
1	Shoreline	shore_orig	vector	shore_orig.gif	shore_orig_meta	various
2	Pierless Shoreline	shoreline	vector	shoreline.gif	shoreline_meta	various
3	DEM (30 m res.)	seattle30	raster	seattle30.gif	seattle30_meta	30
4	DEM (90 m res.)	seattle90	raster	seattle90.gif	seattle90_meta	90
5	DEM with Source Deformation (30 m res.)	def30	raster	def30.gif	def30_meta	30
6	DEM with Source Deformation (90 m res.)	def90	raster	def90.gif	def90_meta	90
7	Source Deformation (30 m res.)	src30	raster	src30.gif	src30_meta	30
8	Source Deformation (90 m res.)	src90	raster	src90.gif	src90_meta	90
9	Maximum Wave Heights	maxh	raster	maxh.gif	maxh_meta	30
10	Maximum Inundation Depths	maxd	raster	maxd.gif	maxd_meta	30
11	Maximum Current Speeds	maxv	raster	maxv.gif	maxv_meta	30
12	Maximum Inundation Depth Lines	inundation	vector	inundation.gif	inundation_meta	30
13	Maximum Inundation Depth Zones	maxd	raster	maxd_zones.gif	maxd_meta	30
14	Maximum Current Speed Zones	maxv	raster	maxh_zones.gif	maxv_meta	30

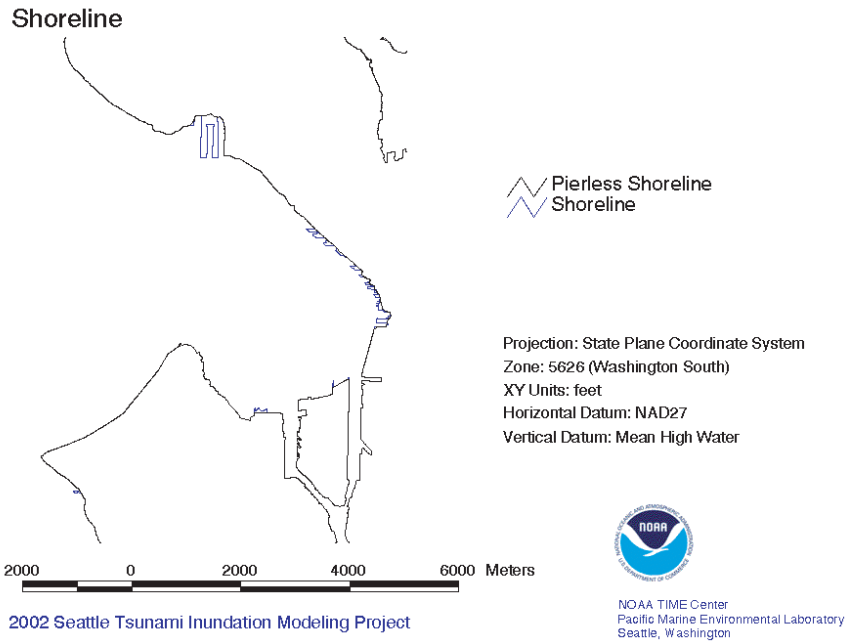

Figure B1: Vector shoreline of the Seattle Area.

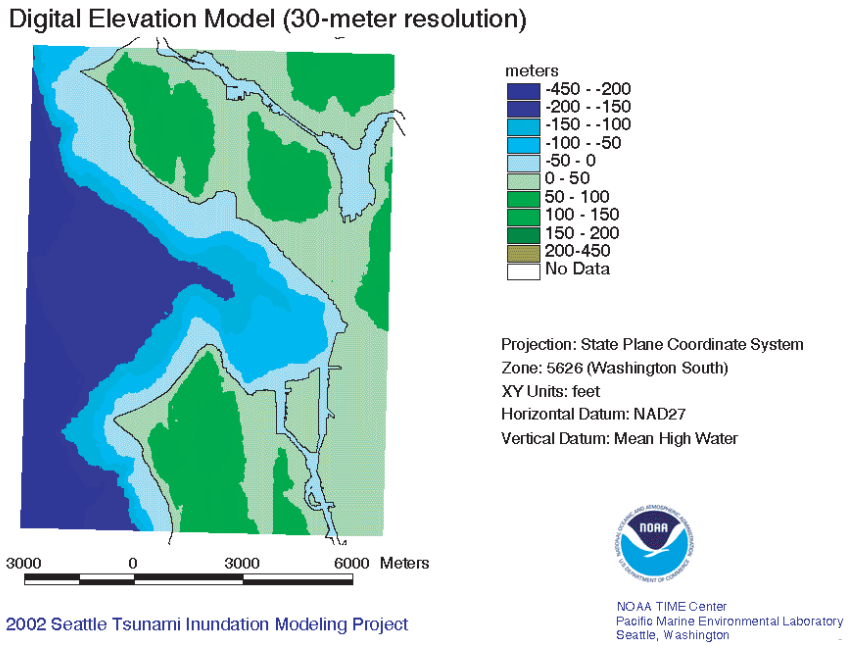

Figure B2: Digital Elevation Model (DEM) for modeling Seattle Area inundation (30 m-resolution).

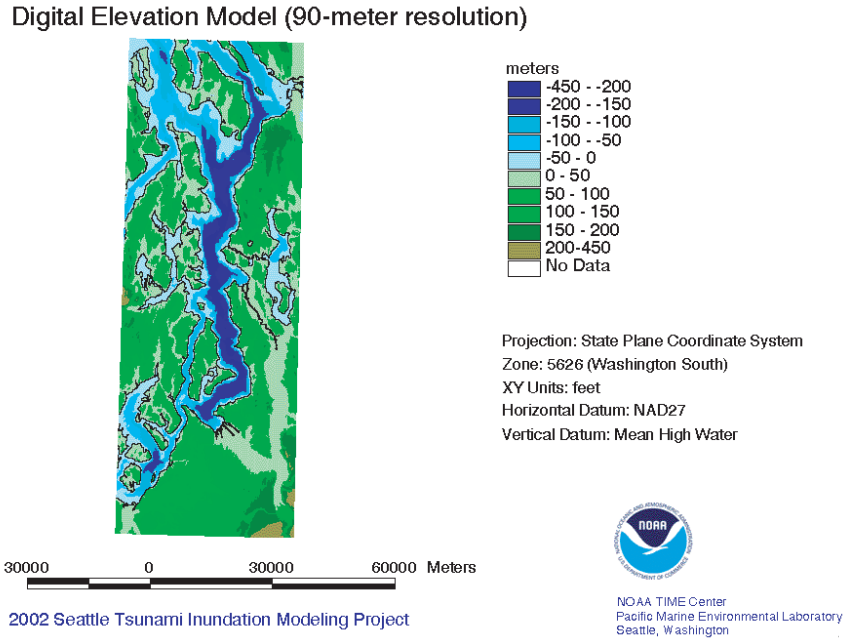

Figure B3: DEM for modeling propagation in Puget Sound (90 m-resolution).

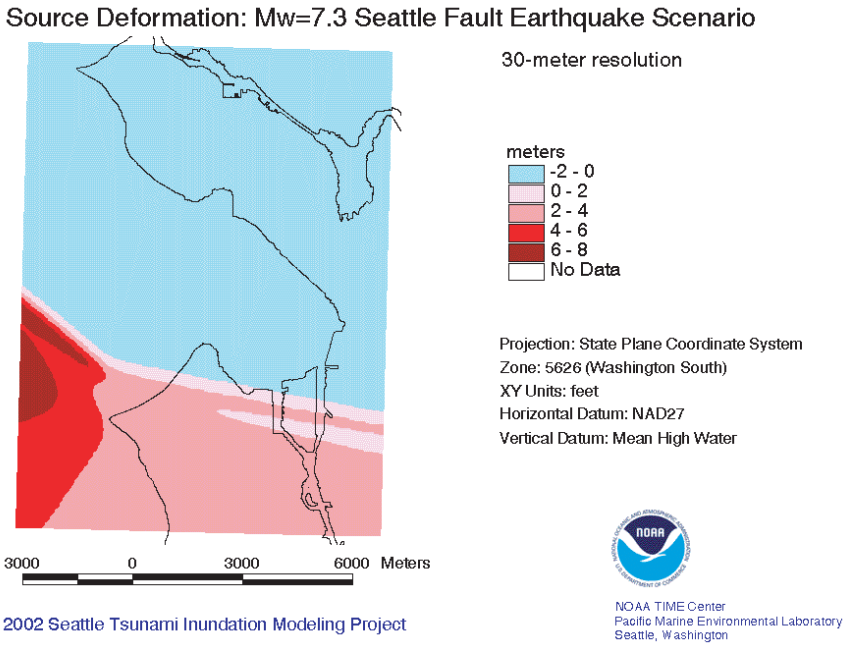

Figure B4: Source deformation for the Seattle 30 m DEM.

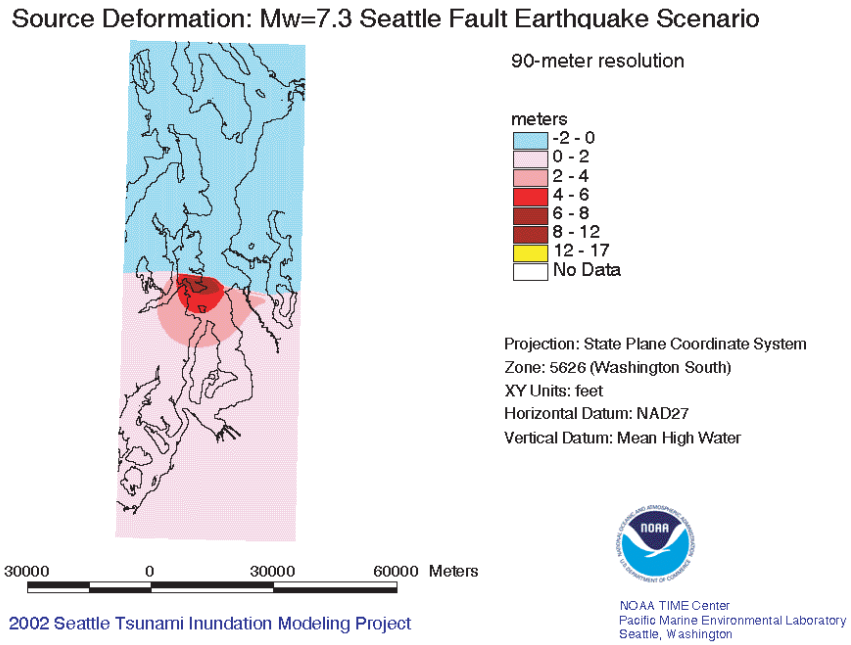

Figure B5: Source deformation for the Puget Sound 90 m DEM.

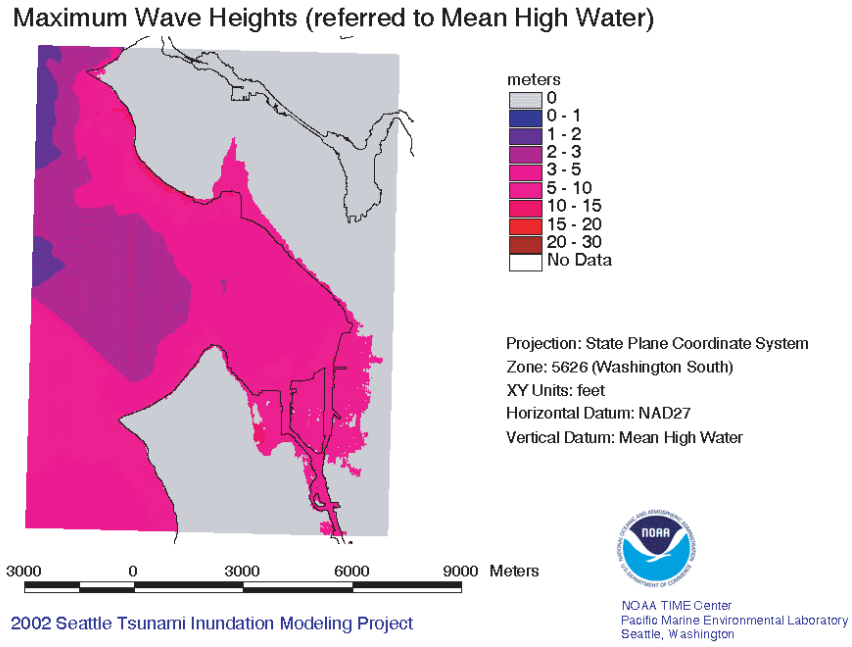

Figure B6: Maximum computed wave heights (measured from Mean High Water) for each node of the Seattle grid.

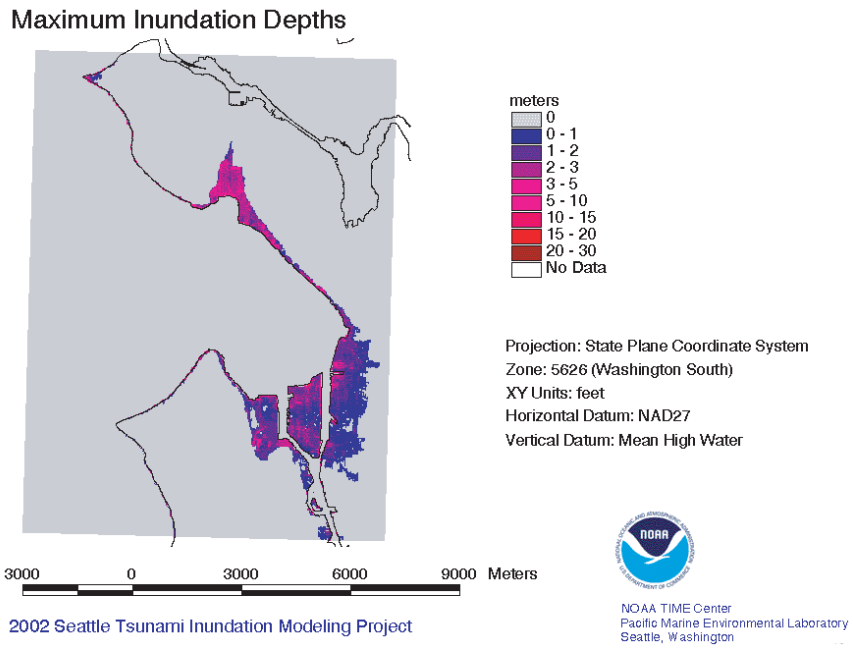

Figure B7: Maximum computed inundation depths (depth of water over land measured from a topography height) for each node of the Seattle grid.

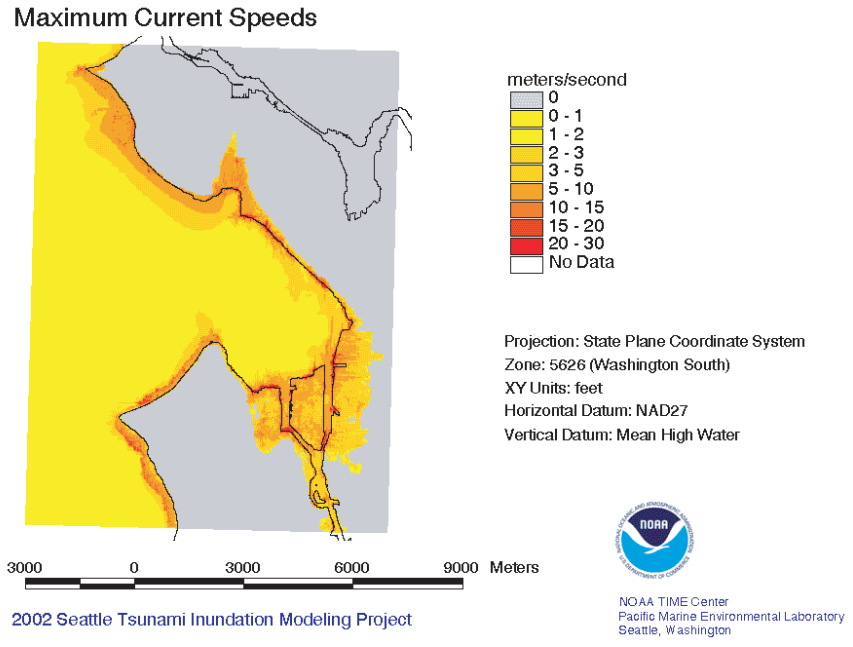

Figure B8: Maximum computed flow velocity (m/s) for each node of the Seattle grid.

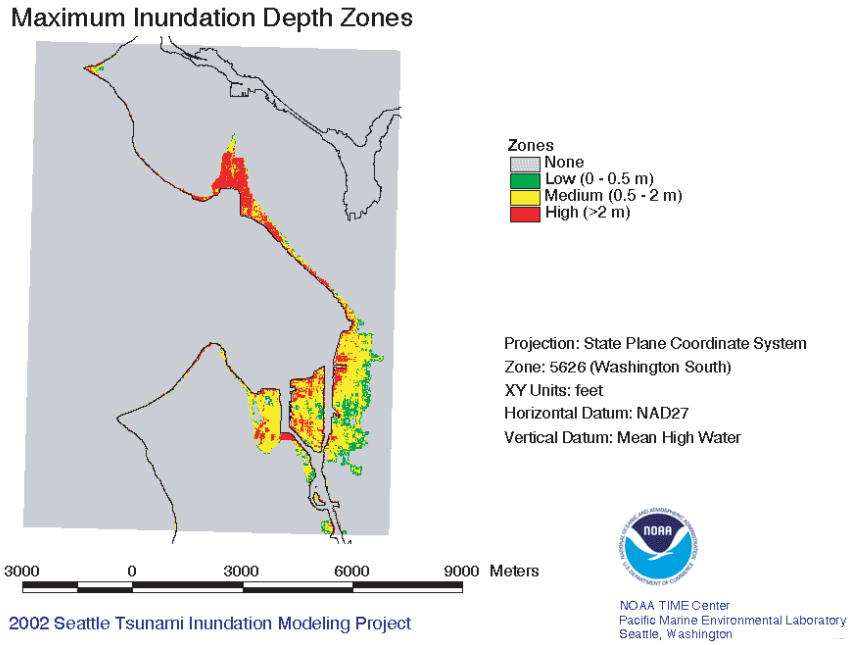

Figure B9: Zones of maximum inundation for the Seattle grid.

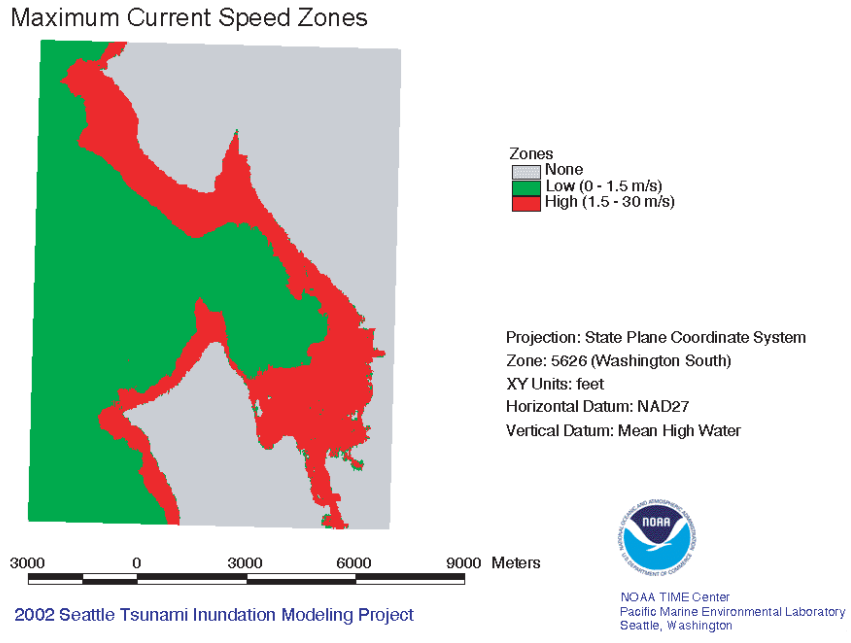

Figure B10: Zones of maximum flow velocity for the Seattle grid.